

## Accepted Manuscript

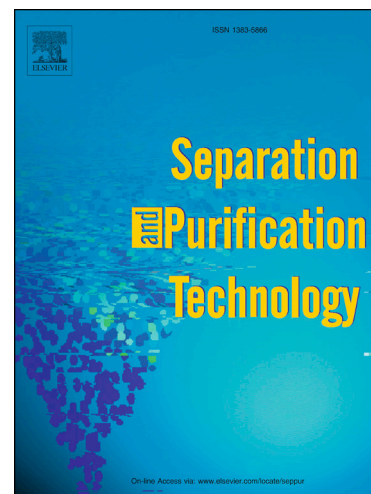
Influence of various experimental parameters on the capacitive removal of phosphate from aqueous solutions using LDHs/AC composite electrodes

Enhao Zhu, Xiaoting Hong, Zhuoliang Ye, K.S. Hui, K.N. Hui

PII: S1383-5866(18)34183-2  
DOI: <https://doi.org/10.1016/j.seppur.2019.01.004>  
Reference: SEPPUR 15234

To appear in: *Separation and Purification Technology*

Received Date: 27 November 2018  
Revised Date: 25 December 2018  
Accepted Date: 3 January 2019



Please cite this article as: E. Zhu, X. Hong, Z. Ye, K.S. Hui, K.N. Hui, Influence of various experimental parameters on the capacitive removal of phosphate from aqueous solutions using LDHs/AC composite electrodes, *Separation and Purification Technology* (2019), doi: <https://doi.org/10.1016/j.seppur.2019.01.004>

This is a PDF file of an unedited manuscript that has been accepted for publication. As a service to our customers we are providing this early version of the manuscript. The manuscript will undergo copyediting, typesetting, and review of the resulting proof before it is published in its final form. Please note that during the production process errors may be discovered which could affect the content, and all legal disclaimers that apply to the journal pertain.

**Influence of various experimental parameters on the capacitive removal of phosphate from aqueous solutions using LDHs/AC composite electrodes**

Enhao Zhu<sup>a, b</sup>, Xiaoting Hong<sup>a,\*</sup>, Zhuoliang Ye<sup>b</sup>, K.S. Hui<sup>c</sup>, K.N. Hui<sup>d</sup>

<sup>a</sup> Department of Chemistry, Zhejiang Sci-Tech University, Hangzhou 310018, China

<sup>b</sup> School of Chemical Engineering, Fuzhou University, Fuzhou, Fujian 350116, P. R.

China

<sup>c</sup> Engineering, Faculty of Science, University of East Anglia, Norwich, NR4 7TJ,

United Kingdom

<sup>d</sup> Institute of Applied Physics and Materials Engineering, University of Macau,

Avenida da Universidade, Taipa, Macau, China

Corresponding author. Tel.: +86 (0571) 86843228, Fax +86 (0571) 86843228.

E-mail address: hanren.xiaoting@gmail.com (X.T. Hong).

**Abstract**

The efficient uptake of phosphate from aqueous solutions was achieved on layered double hydroxides (LDHs)-based electrodes via capacitive desalination in our previous study. The current follow-up work was mainly carried out to study the influence of various experimental parameters on the capacitive removal of phosphate using LDHs/activated carbon (LDHs/AC) composite electrodes. A series of batch experiments were implemented to investigate the experimental factors, including  $\text{Mg}^{2+}/\text{Al}^{3+}$  ratios (2, 3, and 4), trivalent metal cations ( $\text{Al}^{3+}$ ,  $\text{Fe}^{3+}$ ,  $\text{Cr}^{3+}$ ), initial solution pH (from 3 to 10), coexisting anions ( $\text{NO}_3^-$ ,  $\text{Cl}^-$ ,  $\text{SO}_4^{2-}$ ), and ion strengths, in capacitive deionization. The electrode materials before and after capacitive deionization were characterized to reinforce the analysis of the adsorption mechanisms by X-ray powder diffraction, scanning electron microscopy, energy dispersive X-ray, cyclic voltammetry, and electrochemical impedance spectroscopy. Results indicated that the Mg-Al LDHs/AC electrodes exhibited higher phosphate adsorption capacity (80.43 mg  $\text{PO}_4^{3-}/\text{g}$ ), more regular morphology, and higher degree of crystallinity than that of Mg-Fe LDHs/AC and Mg-Cr LDHs/AC. Increasing  $\text{Mg}^{2+}/\text{Al}^{3+}$  ratios enhanced the adsorption capacity of phosphate. The uptake of phosphate by Mg-Al LDHs/AC under circumneutral pH and low ion strength reached the maximum level. Furthermore, the presence of coexisting anions lowered the adsorption capacity of phosphate mainly due to the occurrence of a compressed electrical double layer. Therefore, the influence of different experimental parameters on phosphate removal via capacitive deionization by Mg-Al LDHs/AC necessitates a

systematic investigation to optimize the preparation conditions of LDHs-based electrodes and several important operating parameters.

**Keywords:** Capacitive deionization; Layered double hydroxide; Phosphate removal; Coexisting anion; ion strengths;

## 1. Introduction

The wastewater generated from the production and living processes of humans is directly discharged to water bodies and could result in the severe eutrophication of rivers, lakes, and seas [1]. Untreated wastewater usually contains large amounts of nutrients, such as nitrogen and phosphate for algae growth, resulting in the deterioration of water quality, decrease of dissolved oxygen content and biodiversity, and serious damage to aquatic ecosystems [2]. Phosphate content is recognized as the determining factor for the growth of algae, and thus, excessive phosphate increases the risk of water eutrophication [3]. Therefore, phosphate removal is an urgent requirement in the practical aspect and the basic research aspect.

Capacitive deionization (CDI), a new type of water treatment technology that has been rapidly developed in the past few years, has recently attracted increasing attention [4, 5]. CDI usually consists of two electrodes placed in parallel, as well as an aqueous solution containing ions that flows between or through the charging electrodes. When a certain voltage is applied between the two electrodes, a continuous stable electric field is generated between them; thereafter, the charged ions present in feed water migrate to the electrical double layer (EDL) under the electric field force [6]. During this process, the charged ions (cations and anions) migrate toward the opposite electrode (cathode and anode); consequently, large amounts of ions are strongly electro-adsorbed on the surface of the electrode, leading to a decrease in the salinity of the solution and thereby improving water quality [7-9].

The characteristics of CDI call for an electrode material that has a high specific

surface area, a reasonable pore structure, high hydrophilicity and electrical conductivity, and good chemical stability under high concentrations of water and electricity [10, 11]. CDI capacity is dependent on ion properties; specifically, the capacity of the electrode material is related to not only the specific surface area but also pore size and pore structure [12, 13]. Although micropores can greatly increase the specific surface area of materials, the formed EDL overlaps because the pore size is too small, leading to the reduction of CDI capacity due to the “overlapping effect” [14, 15]. On the contrary, mesopores and macropores are unable to contribute much to the specific surface area; nonetheless, they can provide channels for ion transfer, and their high proportion can greatly improve the ion disappearance effect [16]. In recent years, various carbon materials have been used as CDI electrode materials such as activated carbon (AC). AC which is cheap and easy to obtain has a high specific surface area and a large number of oxygen-containing groups to exhibit an ion capacitive removal activity [17, 18]. However, the performance of AC electrode in phosphate removal tends to be limited [19].

Layered double hydroxides (LDHs), with unique layered structures, are superior materials for anion affinity [20]. Their crystal structure is similar to that of hydrotalcite (with the molecular formula of  $\text{Mg}_{0.75}\text{Al}_{0.25}(\text{OH})_2(\text{CO}_3)_{0.125}\cdot 0.25\text{H}_2\text{O}$ ) in nature. Therefore, LDHs are also called hydrotalcite-like compounds. LDHs can be represented by the general formula  $[\text{M}^{2+}_{1-x}\text{M}^{3+}_x(\text{OH})_2](\text{A}^{n-})_{x/n}\cdot m\text{H}_2\text{O}$ , where  $\text{M}^{2+}$  ( $\text{Mg}^{2+}$ ,  $\text{Ni}^{2+}$ ,  $\text{Co}^{2+}$ ,  $\text{Zn}^{2+}$ ,  $\text{Cu}^{2+}$ , etc.) and  $\text{M}^{3+}$  ( $\text{Al}^{3+}$ ,  $\text{Cr}^{3+}$ ,  $\text{Fe}^{3+}$ ,  $\text{Sc}^{3+}$ , etc.) respectively represent divalent and trivalent metal cations;  $x$  is the molar ratio of  $\text{M}^{3+}/(\text{M}^{2+}+\text{M}^{3+})$ ;

and  $A^{n-}$  is an anion occupying interlayer, such as  $CO_3^{2-}$ ,  $NO_3^-$ ,  $Cl^-$ ,  $SO_4^{2-}$ ,  $PO_4^{3-}$  [21].

Due to the partial substitution of trivalent cations for divalent cations, LDHs have a net positive charge on the layer balanced by intercalated anions in the interlayer and water molecules. Compared with low-valence anions, high-valence interlayer anions have greater affinity with LDHs, resulting in a high layer charge density. As for anion exchange, ions with a small radius are easily introduced to the interlayer of LDHs [22, 23].

LDHs have been widely used in adsorption for their unique anion exchange properties. Stefan Wan et al. [24] prepared a composite material for phosphate adsorption by AC and Mg-Al(Fe) LDH coprecipitation and found that the low phosphate adsorption of Mg-Fe LDH/AC composites is mostly due to the low phosphate affinity of Mg-Fe LDH, which dissolves slower than Mg-Al LDH does. The effects of trivalent metal cations on the CDI process clearly require an in-depth discussion. Li et al. [25] suggested that a large amount of  $Al^{3+}$  would decrease the charge density of mixed metal hydroxide layers and subsequently improve phosphate removal. Das et al. [26] found that the properties and contents of metal cations in LDHs impact the phosphate adsorption capacity and that the maximum phosphate removal occurs at a pH of 5. Competitive anions have adverse effects on adsorption, thereby verifying the notion that anions with higher charge densities have stronger affinity toward LDHs than monovalent anions do. Extensive research has evaluated the effects of coexisting anions. Ultrathin LDH nanosheets for phosphate removal prepared by Zhan et al. [27] are obviously influenced by  $SO_4^{2-}$  due to its strong

affinity to LDH layers.  $\text{Cl}^-$  and  $\text{NO}_3^-$  show a relatively weak influence. Li et al. [25] arrived at the same conclusion, that is,  $\text{SO}_4^{2-}$ ,  $\text{Cl}^-$ , and  $\text{NO}_3^-$  decrease phosphate removal efficiency for different molar ratios of Mg/Al LDH-functionalized biochar. The security of adsorbents is known to perform an important function because many LDHs synthesized with heavy metals could be released into solutions to contaminate the environment. By contrast, Mg-Al LDHs are eco-friendly materials. Wang et al. [28] synthesized LDHs by nucleation and aging phase separation and explained the electrochemical behavior, which suggests that LDHs may be a favorable electrode material for supercapacitors. However, CDI on Mg-Al LDH-based electrodes has yet to be realized. AC can be used as a support material to grow LDHs on its surface to avoid structural collapse and aggregation [29]. AC, as a support frame, can increase the contact area between LDHs and electrolytes, shorten the diffusion distance between ions and electrons, and reduce overall resistance. Recently, Wan et al. [24] prepared a composite material for phosphate adsorption by AC and LDH coprecipitation and established a higher adsorption rate.

CDI is a new type of water treatment technology, and LDHs with characteristics that favor phosphate removal could be a good electrode material. We designed Mg-Al LDHs supported on AC by coprecipitation method and used them as the anode material to remove phosphate by CDI. The main objective is to investigate the relationship between CDI capacity and the ratios of  $\text{M}^{2+}/\text{M}^{3+}$  and that between CDI capacity and different trivalent metal cations. Furthermore, this study seeks to elucidate the effects of initial pH, ionic strength, and coexisting anions on the

phosphate CDI performance of Mg-Al LDHs/AC. All observations mentioned above are aimed at improving the phosphate removal performance of LDHs/AC composite electrodes on the basis of our findings.

## 2. Materials and methods

### 2.1 Materials

All solutions were prepared using deionized water (18.2 M $\Omega$ ·cm). All reagents were of analytical grade and used as received. Graphite flakes were supplied by Qingdao Baofeng Graphite Co., Ltd. Commercial AC provided by TIG Technology Co., Ltd. (Shenzhen, China) was used as the porous support material of the composite electrode. Polyvinylidene difluoride (PVDF) was supplied by Arkema (France). Acetylene black was purchased from Taiyuan Liyuan Co., Ltd.

### 2.2 Experimental

**Electrode material synthesis.** AC (2.00 g) was ultrasonically dispersed into 50 mL of 80% ethanol in a 250 mL beaker for 30 min to obtain a uniform suspension. Then, 100 mL of salt solution containing MgCl<sub>2</sub>·6H<sub>2</sub>O and AlCl<sub>3</sub>·6H<sub>2</sub>O (FeCl<sub>3</sub>·6H<sub>2</sub>O, CrCl<sub>3</sub>·6H<sub>2</sub>O) with a certain molar ratio ( $M^{2+}/M^{3+}=2, 3, \text{ and } 4$ ) was slowly added into the suspension, and the mixture was thoroughly stirred. The pH of the mixture was adjusted to 10 with 3 mol·L<sup>-1</sup> NaOH under vigorous magnetic stirring. Then, the mixture was transferred into an oven and aged at 80 °C for 4 h. The dried solid was washed with deionized water until neutral and dried in an oven at 60 °C overnight. Finally, the product was uniformly ground with agate mortar to obtain the electrode

material labeled as Mg-Al LDHs/AC.

**Electrode preparation.** All electrodes were prepared using the same procedure. The viscous electrode slurry was prepared by adding 1.00 g of mixture of 85 wt% electrode material, 10 wt% acetylene black, and 5 wt% PVDF to N-methyl-2-pyrrolidone (NMP). After homogeneous stirring, the electrode was subsequently prepared by spreading the homogeneous slurry on graphite plates (4.0 cm × 2.5 cm) using a scraper blade. Thereafter, the prepared electrodes were dried at 60 °C overnight to remove the NMP and then sealed for the CDI experiment. Each electrode with a mass of the active material in the range of 0.09–0.11 g was immersed in deionized water before use.

**Capacitive deionization.** A self-made CDI reactor (Fig. 1) comprised two parallel electrode plates. The anode electrode is our as-prepared electrode of LDHs/AC and the cathode electrode is graphite flake without active materials. These two electrode were separated by a non-conductive polytetrafluoroethylene mesh with a gap distance of 2 mm for solution flow. Exactly 100 mL of aqueous solution in the whole system was pumped to the bottom, and it then exited from the top of the CDI module, from which ions were removed and transferred to a recycling bottle by a peristaltic pump with a flow rate of 30 mL/min. A potential of 1.2 V between the two electrodes in these experiments was applied once the solution flows through the electrodes to try to avoid the physical adsorption before the CDI experiments. The pH of the solution was monitored at different intervals by a pH meter (FE20 Plus, Mettler-Toledo, Switzerland). All samples were obtained at different intervals, and the concentrations

of phosphate were analyzed using the ammonium molybdate spectrophotometric method by a continuous flow analyzer (AA3, SEAL, Germany). The adsorption capacity ( $q$ ), defined as the uptake quantity of phosphate ions adsorbed per unit mass of electrode material, was calculated as follows:

$$q = \frac{(C_0 - C_t)V}{m} \quad (1)$$

where  $C_0$  and  $C_t$  (mg/L) are the initial phosphate concentration and phosphate concentration at time  $t$ , respectively;  $V$  (L) is the total volume of the solution; and  $m$  (g) is the mass of the active materials on anode electrode.

The pH of the 250 mg  $\text{PO}_4^{3-}$ /L phosphate solution was adjusted with 1 mol/L HCl,  $\text{HNO}_3$ ,  $\text{H}_2\text{SO}_4$ , and KOH to prepare a series of  $\text{KH}_2\text{PO}_4$  solutions with pH of 3, 5, 7, 8, and 10. The ion strength of the solution with 250 mg  $\text{PO}_4^{3-}$ /L phosphate was adjusted using 0.5 mol/L KCl,  $\text{KNO}_3$ , and  $\text{K}_2\text{SO}_4$  to obtain a series of phosphate solutions with ion strengths of  $I_1=7.5$  mM,  $I_2=15$  mM, and  $I_3=22.5$  mM.

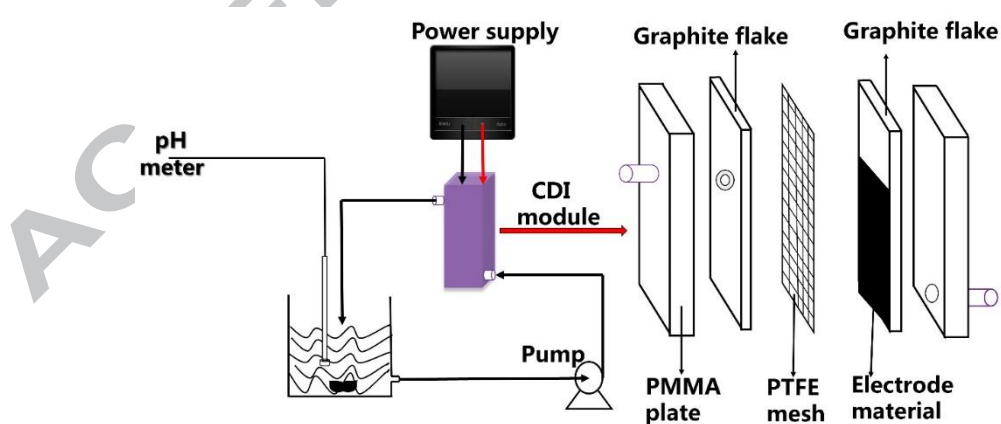


**Fig. 1.** Schematic diagram of CDI process

### 2.3 Analytical methods

X-ray diffraction (XRD) patterns were recorded with a PANalytical X'Pert<sup>3</sup> Powder (Netherlands) diffractometer with monochromatic Cu K $\alpha$  irradiation in the 2 $\theta$  angular regions between 5° and 85° at an operation voltage of 40 kV [30]. The surface morphology and atomic distribution of the electrode materials before and after adsorption were obtained with a scanning electron microscope (SEM, Phenom Pro X, Phenom, Netherlands; FESEM, Nova NanoSEM 230, FEI, USA). Hydrophilicity was estimated using water contact angle measurement by a JY-82 system (DingSheng, China).

Cyclic voltammetry (CV) measurements were performed in a three-electrode cell on an electrochemical workstation (Autolab PGSTAT204). The working electrode is our prepared electrode using LDHs/AC. A graphite plate acted as the counter electrode, and a Ag/AgCl electrode was used as the reference electrode in phosphate solutions at room temperature. The CV curve was obtained in a potential range of -0.2 – 1.2 V with a scan rate of 5 mV/s.

Electrochemical impedance spectra (EIS) tests were performed in a three-electrode cell on an electrochemical workstation (Autolab PGSTAT204). The working electrode is the as-prepared electrode of LDHs/AC. A graphite plate acted as the counter electrode, and a Ag/AgCl electrode was used as the reference electrode in phosphate solutions at room temperature. EIS were conducted to investigate the resistivity of the electrodes and the conductivity at the electrode/electrolyte interface in a frequency range of 1000 kHz to 0.1 Hz and amplitude of 5 mV. The EIS data

were calculated using Nyquist plots, and an equivalent circuit was fitted by ZSimpWin software to obtain the interfacial charge transfer resistance ( $R_{ct}$ ).

### 3. Results and discussion

#### 3.1 Influence of $Mg^{2+}/Al^{3+}$ ratios on phosphate removal by Mg-Al LDHs/AC

The XRD patterns of Mg-Al LDHs/AC materials with different  $Mg^{2+}/Al^{3+}$  ratios are shown in Fig. 2a. Typical hydrotalcite diffraction peaks at lattice planes of (003), (006), (012) and (110) which were consistent with the standard card (PDF #54-1030) as well as weak AC diffraction peaks, were simultaneously present, thereby indicating the successful preparation of the Mg-Al LDHs/AC composite [31]. The excellent multiple relationships between  $d_{003}$  and  $d_{006}$  demonstrated the existence of a unique layered structure. The value of lattice parameters  $a$  ( $=2d_{110}$ ) provides the cation–cation distance within the cationic (octahedral) layer, whereas  $c$  ( $=3d_{003}$ ) is related to the total thickness of the hydroxide (brucite-like) layer and the interlayer distance. The interlayer spaces were obtained by the layer space ( $d_{003}$ ) minus the thickness of the layer (0.48 nm), as listed in Table 1 [32]. The interlayer spaces of the Mg-Al LDHs/AC materials with  $M^{2+}/M^{3+}$  mole ratios of 2, 3, and 4 were 0.3080, 0.3150, and 0.3355 nm, respectively. The content of trivalent metal cation decreased with increasing proportion of  $Mg^{2+}/Al^{3+}$ , resulting in a weak interlayer charge density and high interlayer space [25]. According to the semiquantitative EDX results (Table 1), the loading ratios of  $Mg^{2+}/Al^{3+}$  were 2.38, 3.10, and 4.33; these values are relatively close to the stoichiometric ratios of 2, 3, and 4, respectively.

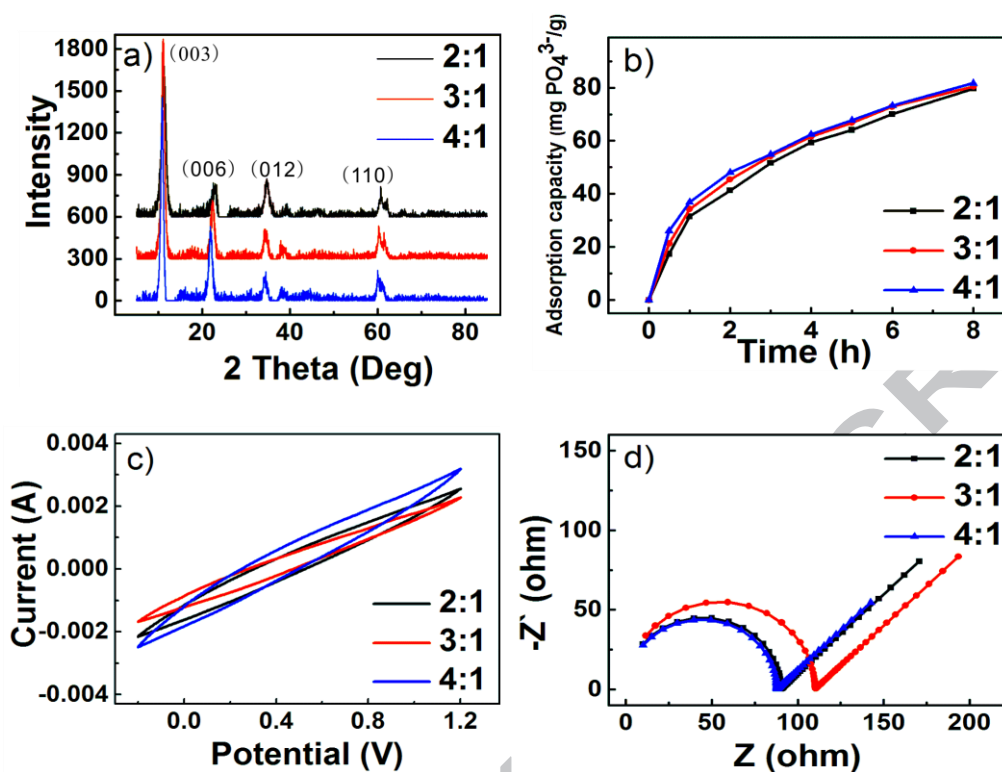


**Fig. 2.** a) XRD patterns, b) effect of contact time on phosphate adsorption, c) CV curves, and d) Nyquist plots of Mg-Al LDHs/AC with different  $Mg^{2+}/Al^{3+}$  ratios.

**Table 1.** Results of XRD and EDX of Mg-Al LDHs/AC and Mg- $M^{3+}$  LDHs/AC

( $M^{3+}=Al^{3+}$ ,  $Fe^{3+}$ , and  $Cr^{3+}$ ).

	XRD					EDX		
	$d_{110}$ (nm)	a(nm)	$d_{003}$ (nm)	c(nm)	Interlayer space(nm)	$d_{006}$ (nm)	Mg(%)	Al(%)
2:1	0.1522	0.3044	0.7838	2.3514	0.3038	0.3847	3.1	1.3
3:1	0.1534	0.3068	0.7950	2.3850	0.3150	0.3945	3.1	1.0
4:1	0.1537	0.3074	0.8155	2.4465	0.3355	0.4059	2.6	0.6
Mg-Al	0.1534	0.3068	0.7950	2.3850	0.3150	0.3945	3.1	1.0
Mg-Fe	0.1554	0.3108	0.8022	2.4066	0.3222	0.4008	3.0	1.1
Mg-Cr	0.1536	0.3072	0.7982	2.3946	0.3182	0.3984	3.3	1.2

**Table 2.** Values of electrochemical parameters of Mg-Al LDH/AC and Mg-M<sup>3+</sup>

	LDH/AC (M <sup>3+</sup> =Al <sup>3+</sup> , Fe <sup>3+</sup> , and Cr <sup>3+</sup> )					
	2:1	3:1	4:1	Mg-Al	Mg-Fe	Mg-Cr
Specific capacitance (F/g)	0.66	0.66	0.65	0.19	0.18	0.22
R <sub>ct</sub> (ohm)	102.5	108.7	102.4	110.0	112.0	118.7

CV and EIS were carried out to investigate the electrochemical properties of Mg-Al LDHs/AC with different Mg<sup>2+</sup>/Al<sup>3+</sup> ratios shown in Fig. 2c and 2d. No obvious redox peak was observed in the CV curves, thereby indicating that Faraday reaction was absent at the electrode interface to avoid the fluctuations in the effluent water quality[33, 34], and the EDL capacitance generated by the Coulomb reaction. The shape of CV deviated from the rectangular due to the resistivity of the phosphate solution and decreased charging speed[35]. The area of the closed CV curve could be used to evaluate specific capacitance [36], and the Nyquist spectrum was fitted to obtain the interfacial charge transfer resistance ( $R_{ct}$ ) by an approximate equivalent circuit for the CDI process. The results are shown in Table 2. The specific capacitances of 2:1, 3:1, and 4:1 Mg-Al LDHs/AC were calculated as 0.66, 0.66, and 0.65 F/g, respectively, using the following equation:

$$C = \frac{\int IdV}{2mv\Delta V} \quad (2)$$

where  $C$  is the specific capacitance,  $\int IdV$  is the area of the closed CV curve,  $m$  is the mass of the active materials in anode electrode,  $v$  is the scan rate of CV, and  $\Delta V$  is the potential range.

The values of  $R_{ct}$  were calculated as 102.5, 108.7, and 102.4 ohm for 2:1, 3:1, and 4:1 Mg-Al LDH/AC, respectively. Based on the CV and EIS results, the specific capacitances and the values of  $R_{ct}$  of 2:1, 3:1 and 4:1 Mg-Al LDHs/AC were similar. The difference of adsorption capacities would be mainly influenced by chemical adsorption via phosphate intercalation and surface complexation on the active materials rather than electric double layer. Furthermore, the difference between without and with applied potential on the 3:1 MgAl-LDHs/AC capacity of phosphate (50.12 mg  $PO_4^{3-}$ /g vs 80.43 mg  $PO_4^{3-}$ /g) also indicates electric double layer would not be the major factor on phosphate removal.

The effects of contact time on the phosphate adsorption by Mg-Al LDHs/AC electrodes with  $M^{2+}/M^{3+}$  ratios of 2, 3, and 4 are shown in Fig. 2b. The adsorption rate in the initial 2 h dramatically increased to 41.29, 45.39, and 48.03 mg  $PO_4^{3-}$ /g mainly due to the electrostatic adsorption and EDL adsorption of the positively charged surface of the adsorbent and the negatively charged phosphate. The subsequent adsorption at a relatively slow rate indicated the progressive saturation of available adsorption sites, which possibly induced repulsive forces among the adsorbed phosphates on the surface [37]. The adsorption amount increased with the increasing contact time. The adsorption capacities of Mg-Al LDH/AC with  $M^{2+}/M^{3+}$  mole ratios of 2, 3, and 4 in 8 h were 79.59, 80.43, and 81.69 mg  $PO_4^{3-}$ /g, respectively. The phosphate adsorption amount of Mg-Al LDHs/AC without an applied potential mentioned in R.H. Li's research is 17 mg P/g (calculated about 51 mg  $PO_4^{3-}$ /g)[24]. The results showed that phosphate removal capability could be dramatically enhanced

under an applied voltage. The phosphate uptake amount increased with the increase of the ratios of  $M^{2+}/M^{3+}$ . The Mg-Al LDHs/AC with a  $M^{2+}/M^{3+}$  ratio of 4 was of a large interlayer space and loose interlayer structure, as shown in previous XRD results. These properties facilitated the entry of phosphate into the interlayer adsorption site and its intercalation into the LDHs layer. The inner-sphere complexes between phosphate and Mg-O during the process of phosphate adsorption were a dominant mechanism [38]. Moreover, the content of Mg-O increased with a high ratio of  $Mg^{2+}/Al^{3+}$ . The complexation sites increased accordingly, and the adsorption capacity of phosphate was obviously enhanced. As the Fig. 2b. shown, the phosphate removal between different  $Mg^{2+}/Al^{3+}$  ratios of Mg-Al LDHs/AC have a small difference. The results were in accordance with the previous studies [25]. It would be caused by a close interlayer space (Table 1.) and water contact angle (Fig.5.).

### 3.2 Influence of different $M^{3+}$ on phosphate removal by Mg- $M^{3+}$ LDHs/AC

The XRD spectra of Mg- $M^{3+}$  LDHs/AC ( $M^{3+}=Al^{3+}$ ,  $Fe^{3+}$  and  $Cr^{3+}$ ) materials shown in Fig. 3a indicated that the typical hydroxalite diffraction peaks at (003), (006), (012) and (110) were correlated with the LDHs and weak diffraction peak of AC [31]. The excellent multiple relationships between  $d_{003}$  and  $d_{006}$  demonstrated the existence of a unique layered structure. The relatively weak characteristic diffraction peaks of the Mg-Cr LDHs/AC material indicated its low degree of crystallinity. Comparatively, Mg-Al LDHs/AC possessed the best crystallinity. The cell parameters and interlayer spaces were calculated according to  $a=2d_{110}$ ,  $c=3d_{003}$ , and the layer

space  $d_{003}$  equivalent to the sum of the interlayer space and the thickness of the layer (0.48 nm) [32]. The results are listed in Table 1. Parameter  $a$  is related to the distance between cations. The large radii of the trivalent metal cation serving as the isomorphous substitute of  $Mg^{2+}$  resulted in the large value of parameter  $a$ . Given the ionic radii of  $Al^{3+}$ ,  $Cr^{3+}$ , and  $Fe^{3+}$  being 0.051, 0.061, and 0.065 nm, respectively, the values of parameter  $a$  were equal to 0.3068, 0.3072, and 0.3108 nm, respectively [39].

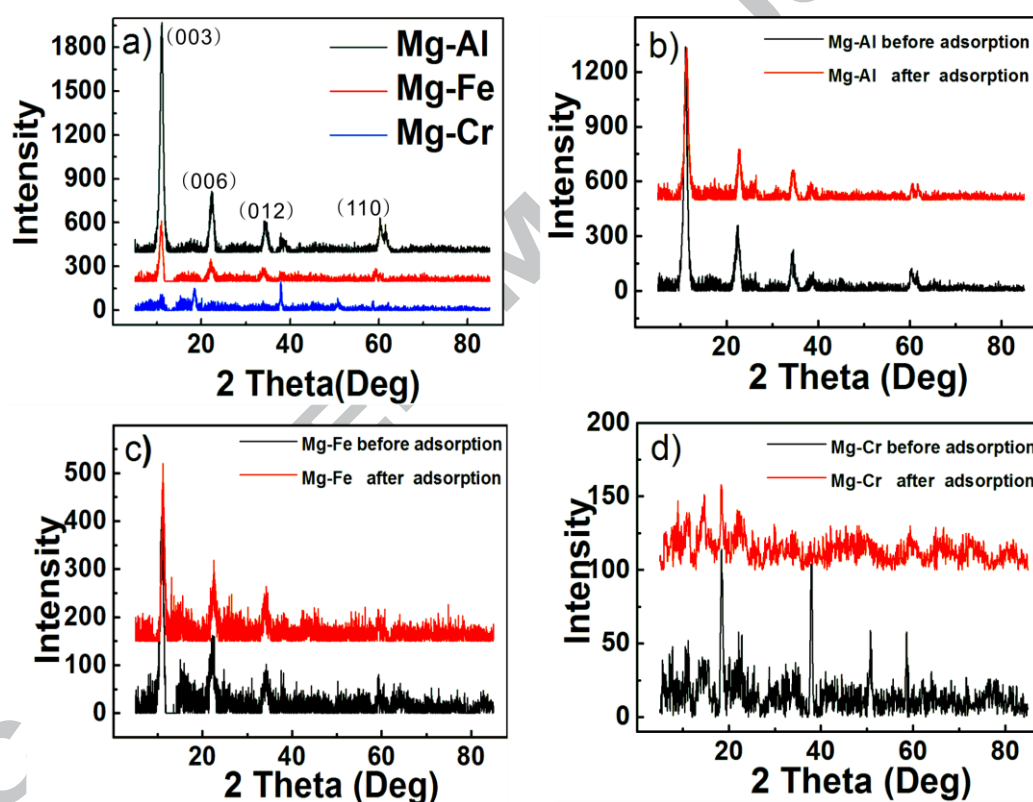


**Fig. 3.** XRD patterns of a)  $Mg-M^{3+}$  LDHs/AC materials and b), c), d)  $Mg-M^{3+}$  LDHs/AC electrodes before and after capacitive desalination ( $M^{3+}=Al^{3+}$ ,  $Fe^{3+}$ , and  $Cr^{3+}$ ).

The morphology images of  $Mg-M^{3+}$  LDHs/AC ( $M^{3+}=Al^{3+}$ ,  $Fe^{3+}$  and  $Cr^{3+}$ ) in Fig.

4 clearly presented the bright particles corresponded to the LDHs deposited on the surface of AC within the matrix. The Mg-Al and Mg-Fe LDHs/AC materials had obviously large LDHs particles. The Mg-Cr LDHs/AC material comprised LDHs particles with relatively heterogeneous size and shape.

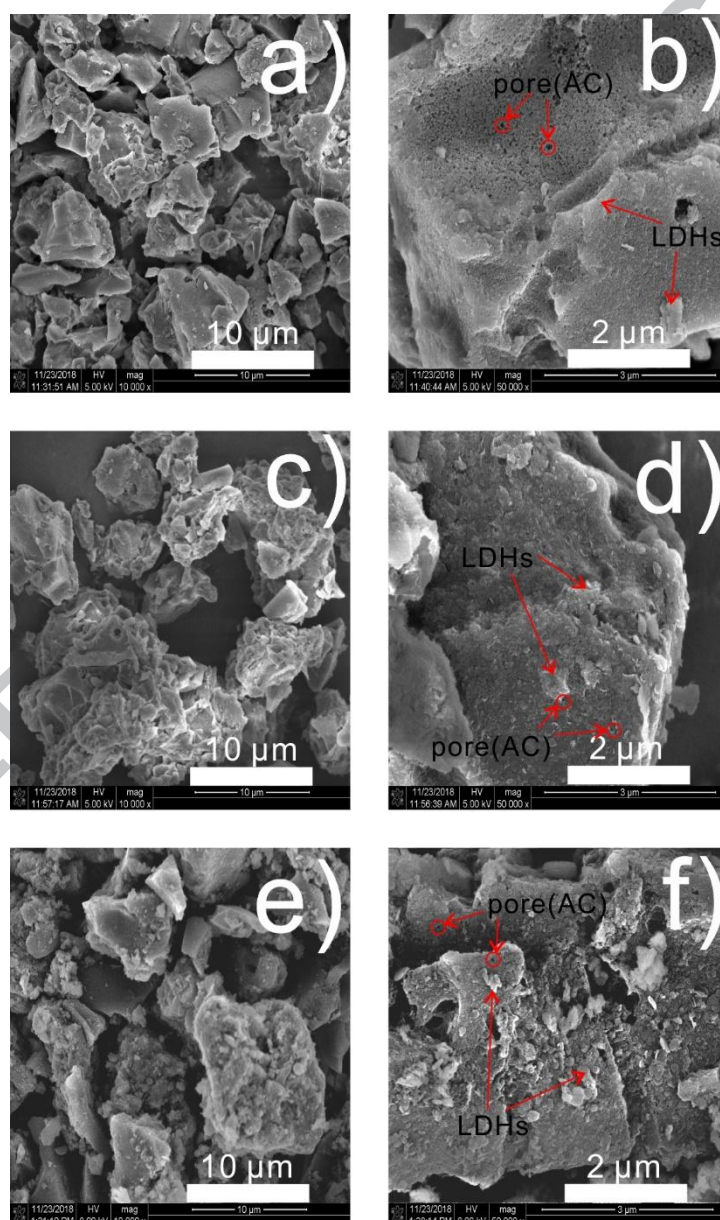


**Fig. 4.** SEM images of Mg- $M^{3+}$  LDHs/AC  $M^{3+}$ =a), b)  $Al^{3+}$ ; c), d)  $Fe^{3+}$ ; and e), f)

$Cr^{3+}$ .

To study the wettability of the LDHs/AC composite electrodes, the optical micrographs of the dynamic water contact angle experiments on the surface of electrodes as a function of contact time have provided as Fig. 5. The contact angle of Mg-Cr LDHs/AC is  $137^\circ$  at 90 s which is larger than other electrodes. These results indicated that Mg-Cr LDHs/AC possess the worst hydrophilicity of the LDHs/AC composite electrodes [40, 41].

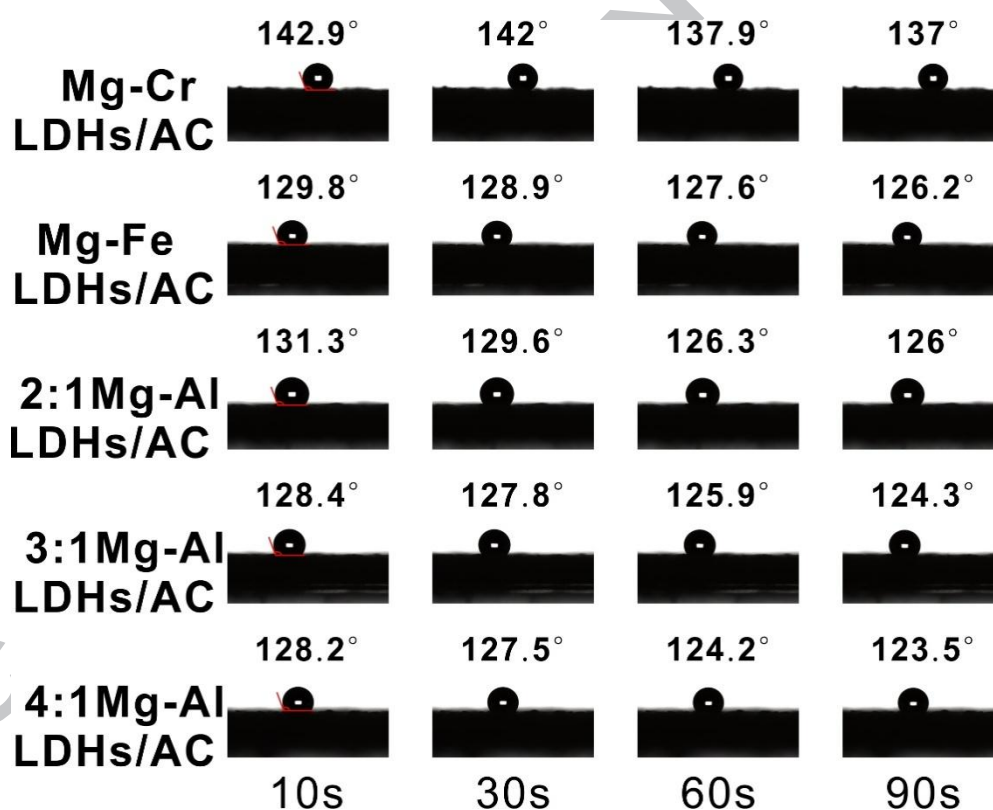
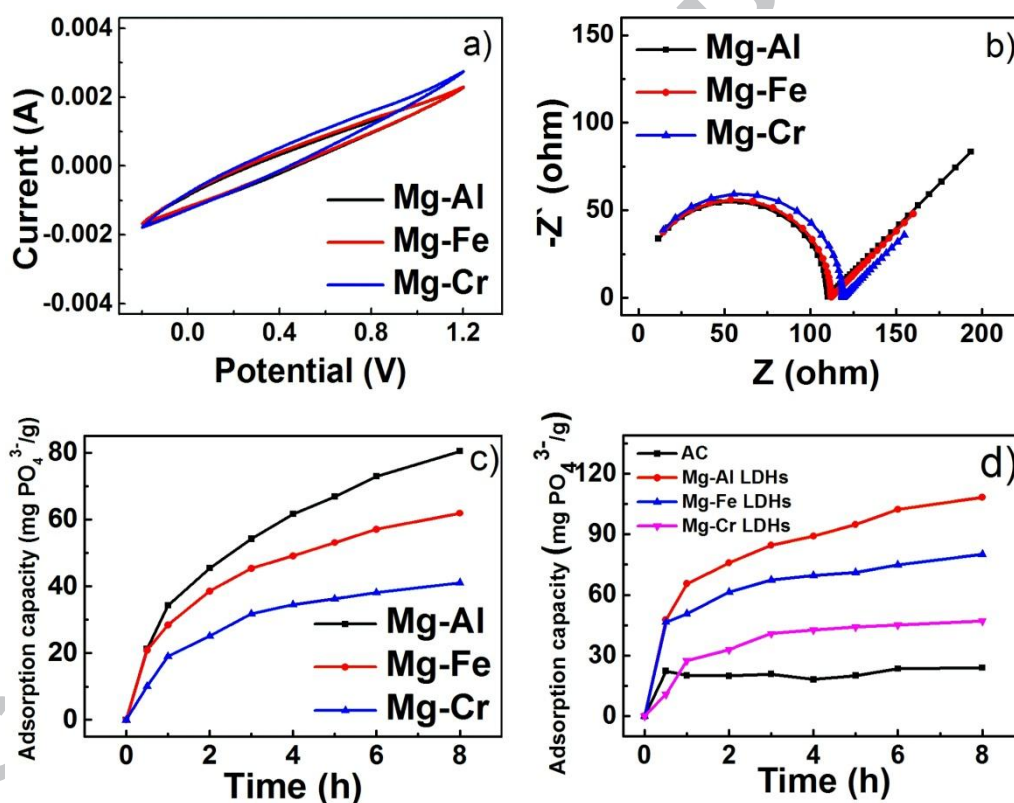


Fig. 5. Dynamic water contact angle analysis of Mg- $M^{3+}$  LDHs/AC ( $M^{3+}=Al^{3+}$ ,  $Fe^{3+}$ , and  $Cr^{3+}$ ).

CV and EIS were performed to study the electrochemical properties of different

$M^{3+}$  LDH/AC materials. The curves shown in Fig. 6a indicated that a typical EDL capacitor formed on the electrode surface. The calculated results are shown in Table 2. The specific capacitances of Mg-Al, Mg-Fe, and Mg-Cr LDHs/AC were 0.19, 0.18, and 0.22 F/g, respectively; and the values of  $R_{ct}$  were 110.0, 112.0, and 118.7 ohm, respectively. This result indicated that the charge transfer resistance in Mg-Al LDHs/AC was less than that in the other electrodes.



**Fig. 6.** a) CV curves; b) Nyquist plots; effects of contact time on the phosphate adsorption of c) Mg-M<sup>3+</sup> LDHs/AC (M<sup>3+</sup>=Al<sup>3+</sup>, Fe<sup>3+</sup>, and Cr<sup>3+</sup>) and d) AC and pure Mg-M<sup>3+</sup> LDHs (M<sup>3+</sup>=Al<sup>3+</sup>, Fe<sup>3+</sup>, and Cr<sup>3+</sup>).

As indicated by the increment of the adsorption amount of phosphate by Mg-M<sup>3+</sup>

LDHs/AC of different  $M^{3+}$  (Fig. 6c), the adsorption rate was considerably fast in the initial adsorption stage due to the EDL and electrostatic adsorption. The subsequent adsorption amounts of Mg-Al, Mg-Fe, and Mg-Cr LDHs/AC slowly increased to 80.43, 66.86, and 41.09 mg  $PO_4^{3-}$ /g after 8 h, respectively. Kostas S. Triantafyllidis has synthesized a series of LDHs which is partial or complete replaced of  $Al^{3+}$  with  $Fe^{3+}$  ( $Mg_3Al-CO_3$  LDHs,  $Mg_3Fe(III)_{0.4}Al_{0.6}-CO_3$  LDHs,  $Mg_3Fe(III)_{0.8}Al_{0.2}-CO_3$  LDHs,  $Mg_3Fe(III)-CO_3$  LDHs). Replacement of Al(III) by Fe(III) in the LDH samples containing carbonates led to a small decrease in sorption efficiency, indicating a stronger bonding of carbonates due to the presence of Fe(III). The enhanced affinity between Mg-Fe LDHs/AC and carbonates as charge-balancing anions, relative to the affinity between Mg-Al LDHs/AC and carbonates, led to a low phosphate adsorption capacity [42]. The worst crystallinity of Mg-Cr LDHs/AC could deteriorate the intercalation of phosphate in the interlayer of LDHs and thus lead to poor adsorption. Based on our experimental results, the phosphate adsorption amount on the pristine activated carbon electrode is  $\sim 20.85$  mg  $PO_4^{3-}$ /g. The electro-sorption performance of pure AC, Mg-Al LDHs, Mg-Fe LDHs, and Mg-Cr LDHs electrodes compared as Fig. 6d showed that the LDH-containing electrodes possess a much better capacity (108.15, 80.12, and 47.15 mg  $PO_4^{3-}$ /g) than that of the pure AC electrode (20.85 mg  $PO_4^{3-}$ /g) which indicate that LDH play important roles in phosphate removal than supporters. The apparent adsorption capacity of the composites was lower than pure LDHs. However, the adsorption capacity per unit weight of LDHs in LDHs/AC was higher than that of pure LDHs after uniformed the weight of LDHs.

The XRD patterns of Mg-M<sup>3+</sup> LDHs/AC before and after capacitive desalination are shown in Fig. 3 b–d. They indicated that the intensity of the characteristic diffraction peaks of the three different materials weakened after adsorption, thereby proving that the adsorption resulted in the loss of crystallinity. The basal spacing of LDHs shares a remarkable linear relationship with the size of hydrated intercalated anions. In this study, the  $d_{003}$  values of Mg-Al, Mg-Fe, and Mg-Cr LDH/AC decreased from 0.7979, 0.8008, and 0.7852 nm to 0.7796, 0.7879, and 0.7743 nm after adsorption, respectively. The obtained LDHs contained CO<sub>3</sub><sup>2-</sup> in the interlayer space without obvious incorporation of chloride anions due to the existence CO<sub>2</sub> in air and CO<sub>3</sub><sup>2-</sup> in deionized water and strong interaction between CO<sub>3</sub><sup>2-</sup> and metal ions on the basal [43]. The carbonates in the interlayer were partially replaced by phosphate for the intercalated ion exchange of LDHs, although the effective hydrated ion radius of carbonate (0.39 nm) was slightly smaller than that of phosphate (0.49 nm) [44, 45]. Phosphate had a high electronegativity and a strong hydrogen bond, and these properties effectively lowered the interlayer space of LDHs through the orientation tilt of phosphate ions [46].

### 3.3 Influence of initial solution pH on phosphate removal on Mg-Al LDHs/AC

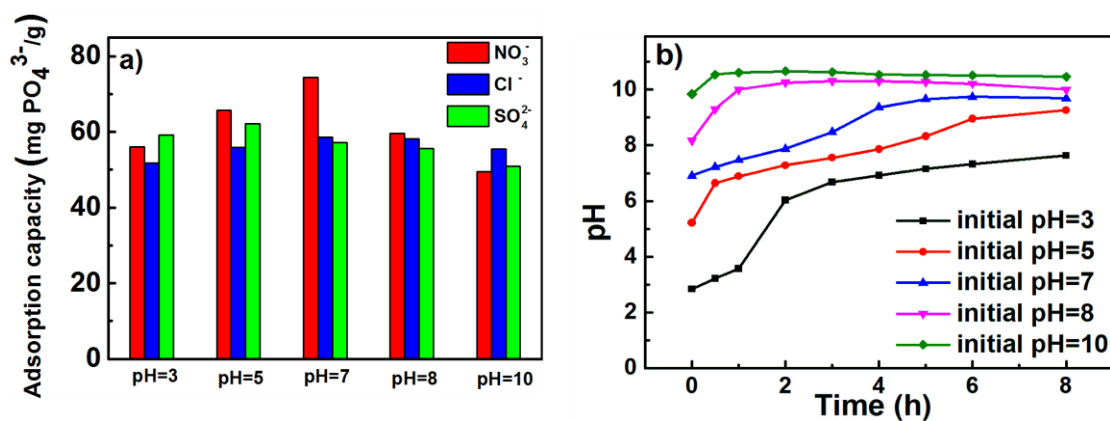


**Fig. 7.** a) Effects of initial pH on phosphate adsorption capacity,

and b) solution pH vary with the electrosorption time at different initial pH.

Generally, the effects of pH are important in the interaction between Mg-Al LDHs/AC and phosphate. That is, the surface charge of Mg-Al LDHs/AC and the main species of phosphate changed with different pH levels. The effects of different initial pH levels on the amount of phosphate adsorbed are shown in Fig. 7a. In the presence of NO<sub>3</sub><sup>-</sup>, Cl<sup>-</sup>, and SO<sub>4</sub><sup>2-</sup>, the maximum adsorption amounts reached 74.46 mg PO<sub>4</sub><sup>3-</sup>/g (pH 7), 58.61 mg PO<sub>4</sub><sup>3-</sup>/g (pH 7), and 62.12 mg PO<sub>4</sub><sup>3-</sup>/g (pH 5), respectively; thus, the ideal initial pH value was 5–7. The adsorption effect of Mg-Al LDHs/AC declined because LDHs dissolve in a low pH solution to destroy the layered structure [47]. Moreover, under pH < p*H*<sub>zpc</sub>, the surface of Mg-Al LDHs/AC was positively charged due to protonation, and it favored the uptake of negative ions by electrostatic attraction. Above pH > p*H*<sub>zpc</sub>, the surface of Mg-Al/LDHs was negatively charged due to deprotonation, and the electrostatic repulsion with negative ions reduced the adsorption amount [48, 49]. The solution pH as a function of electrosorption time at different initial pH is depicted in Fig. 7b. An increase in solution pH with phosphate adsorption was caused by the release of hydroxyl groups into solution which resulted

from the protonation of the surface of Mg-Al LDHs/AC. When the initial pH>8, the decreased solution pH could be explained by the deprotonation of Mg-Al/LDHs due to the solution pH >pH<sub>zpc</sub> after 4 h. The release of H<sup>+</sup> reduced the adsorption amount owing to the electrostatic repulsion.

Different molecular forms of phosphate exist in different pH solutions, as shown by formulas (2–4). When pH is in the range of 2.1–7.2, the main species is H<sub>2</sub>PO<sub>4</sub><sup>-</sup>. When pH is in the range of 7.2–12.3, the dominant ion form is HPO<sub>4</sub><sup>2-</sup>. However, the adsorption free energy of H<sub>2</sub>PO<sub>4</sub><sup>-</sup> is lower than that of HPO<sub>4</sub><sup>2-</sup>, making H<sub>2</sub>PO<sub>4</sub><sup>-</sup> more easily adsorbed on the surface of the adsorbent than HPO<sub>4</sub><sup>2-</sup> [38, 49]. When pH > 7, the OH<sup>-</sup> content in the solution increases with increasing pH, and the existing OH<sup>-</sup> strongly competes with PO<sub>4</sub><sup>3-</sup> to enter the interlayer and adsorption sites of LDHs [50]; hence, a high pH is not conducive to the adsorption of phosphate.

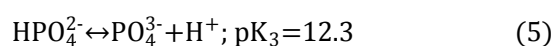
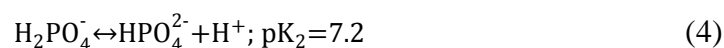
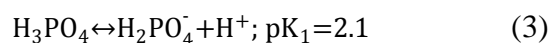


**Table 3.** Specific capacitances of Mg-Al LDHs/AC in different pH levels.

	Specific capacitance (F/g)		
	pH 3	pH 7	pH 10
NO <sub>3</sub> <sup>-</sup>	1.88	3.00	2.03
Cl <sup>-</sup>	2.10	2.62	1.94
SO <sub>4</sub> <sup>2-</sup>	1.71	2.20	2.09

CV was performed on  $\text{KH}_2\text{PO}_4$  solutions containing  $\text{NO}_3^-$ ,  $\text{Cl}^-$ , and  $\text{SO}_4^{2-}$  with an initial solution concentration of 250 mg/L at pH levels of 3, 7, and 10, respectively. As shown in Table 3, the strong acid and strong alkaline solutions exerted a negative effect on capacitance in the pH range of 3–10. In summary, the phosphate adsorption in Mg-Al LDHs/AC included characteristic adsorption, electrostatic adsorption, and EDL adsorption. Moreover, the extremely high or low pH had an adverse effect on adsorption capacity. The phosphate removal on Mg-Al LDHs/AC was related to a wide range of pH.

### 3.4 Effects of coexisting anions and ion strength

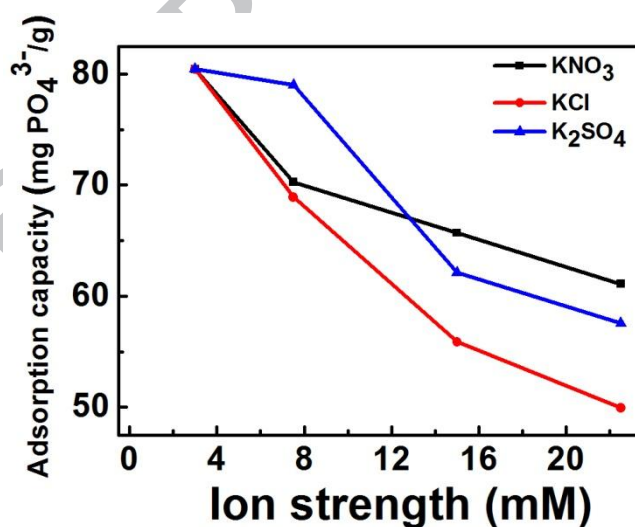


**Fig. 8.** Effects of ionic strengths and coexisting anions on the capacitive uptake of phosphate.

The presence of common anions in water, including  $\text{Cl}^-$ ,  $\text{SO}_4^{2-}$ ,  $\text{NO}_3^-$ , and so on,

has a potential effect on phosphate removal due to competitive adsorption. Fig. 8 shows the effects of different ion strengths and coexisting anions on the uptake amount of phosphate. Adsorption capacity decreased sharply with increasing ionic strength. When the ionic strength of phosphate solution with  $\text{Cl}^-$ ,  $\text{SO}_4^{2-}$ , and  $\text{NO}_3^-$  increased to 22.5 mM, the uptake amount of phosphate decreased from 80.43 mg  $\text{PO}_4^{3-}/\text{g}$  to 49.93, 57.57, and 61.09 mg  $\text{PO}_4^{3-}/\text{g}$ , respectively. Obviously, the competitive adsorption of phosphate reduced the adsorption capacity in the presence of  $\text{Cl}^-$ ,  $\text{SO}_4^{2-}$ , and  $\text{NO}_3^-$ . At the same time, due to the increased ionic strength, the electric field could not spread to a long distance because the solution with a high ionic strength was enough to hold the charge; therefore, the EDL was compressed, and the adsorption capacity decreased [51]. The result suggested that the thickness of the EDL was highly correlated with ionic strength. Although the effects of coexisting ions on phosphate adsorption without applied potential followed the order of  $\text{SO}_4^{2-} > \text{NO}_3^- > \text{Cl}^-$ , which indicated a great agreement with the conclusion from the study [25], Pugazhenthiran et al. [52] implied that the ability of EDL adsorption follows the order of  $\text{Cl}^- > \text{NO}_3^- > \text{SO}_4^{2-}$  during capacitive deionization. The outer-sphere complexation formed is a dominant action as the adsorption capacity of phosphate decreases with increasing ionic strength [53]. Therefore, we can conclude that ionic strength mainly affected the adsorption capacity contributed by the EDL, finally resulting in a decrease in the adsorption capacity of phosphate. The presence of the coexisting ion of  $\text{Cl}^-$  showed the most obvious impact on the adsorption of phosphate, which rapidly decreased with the increase of ionic strength (Fig. 8).

#### 4. Conclusion

The effects of different experimental parameters on phosphate removal via capacitive desalination on LDHs-based electrodes were systematically investigated. A slight increase in the adsorption capacity of phosphate was observed as the  $\text{Mg}^{2+}/\text{Al}^{3+}$  ratios increased because the increase facilitated the entry of phosphate into the adsorption sites, weakened the interlayer charge density, and increased the interlayer space. The influence of different  $\text{M}^{3+}$  on phosphate removal by Mg- $\text{M}^{3+}$  LDHs/AC followed the order of Mg-Al LDHs/AC > Mg-Fe LDHs/AC > Mg-Cr LDHs/AC. Mg-Al LDHs/AC exhibited a high phosphate adsorption capacity (80.43 mg  $\text{PO}_4^{3-}/\text{g}$ ), which was much higher than those recorded in previous studies on phosphate removal by Mg-Al LDHs-based materials. The uptake of phosphate by Mg-Al LDHs/AC could reach the maximum level under circumneutral pH and low ion strength. Furthermore, the presence of coexisting anions lowered the capacitive adsorption of phosphate, and  $\text{Cl}^-$  showed the highest impact on the uptake amount due to the influence of the EDL. Therefore, this study provides effective parameters and conditions for the potential application of LDHs-based electrodes to phosphate removal via capacitive desalination.

#### Acknowledgements

Financial support for this work was provided by Natural Science Foundation of Zhejiang Province (Y18E080055), National Natural Science Foundation of China

(Grant No. 21506037), and the Fuzhou University Qishan Scholar (Oversea project, Grant No. XRC-1508).

## References

- [1] P.J.A. Withers, E.I. Lord, Agricultural nutrient inputs to rivers and groundwaters in the UK: policy, environmental management and research needs, *Sci. Total Environ.*, 282-283 (2002) 9-24.
- [2] L. Håkanson, A.C. Bryhn, J.K. Hytteborn, On the issue of limiting nutrient and predictions of cyanobacteria in aquatic systems, *Sci. Total Environ.*, 379 (2007) 89-108.
- [3] R.C. Nijboer, P.F.M. Verdonchot, Variable selection for modelling effects of eutrophication on stream and river ecosystems, *Ecological Modelling*, 177 (2004) 17-39.
- [4] M.A. Anderson, A.L. Cudero, J. Palma, Capacitive deionization as an electrochemical means of saving energy and delivering clean water. Comparison to present desalination practices: Will it compete?, *Electrochim. Acta*, 55 (2010) 3845-3856.
- [5] Z. Wang, T.T. Yan, G.R. Chen, L.Y. Shi, D.S. Zhang, High Salt Removal Capacity of Metal-Organic Gel Derived Porous Carbon for Capacitive Deionization, *Acs Sustainable Chemistry & Engineering*, 5 (2017) 11637-11644.
- [6] M.E. Suss, S. Porada, X. Sun, P.M. Biesheuvel, J. Yoon, V. Presser, Water desalination via capacitive deionization: what is it and what can we expect from it?, *Energy Environ. Sci.*, 8 (2015) 2296-2319.
- [7] T. Kim, J.E. Dykstra, S. Porada, A. van der Wal, J. Yoon, P.M. Biesheuvel, Enhanced charge efficiency and reduced energy use in capacitive deionization by increasing the discharge voltage, *J. Colloid Interface Sci.*, 446 (2015) 317-326.

- [8] W. Tang, J. Liang, D. He, J. Gong, L. Tang, Z. Liu, D. Wang, G. Zeng, Various cell architectures of capacitive deionization: Recent advances and future trends, *Water Res.*, 150 (2019) 225-251.
- [9] C. Tan, C. He, W.W. Tang, P. Kovalsky, J. Fletcher, T.D. Waite, Integration of photovoltaic energy supply with membrane capacitive deionization (MCDI) for salt removal from brackish waters, *Water Res.*, 147 (2018) 276-286.
- [10] S. Porada, R. Zhao, A. van der Wal, V. Presser, P.M. Biesheuvel, Review on the science and technology of water desalination by capacitive deionization, *Progress in Materials Science*, 58 (2013) 1388-1442.
- [11] H.Y. Duan, T.T. Yan, G.R. Chen, J.P. Zhang, L.Y. Shi, D.S. Zhang, A facile strategy for the fast construction of porous graphene frameworks and their enhanced electrosorption performance, *Chem. Commun.*, 53 (2017) 7465-7468.
- [12] R. Zhao, P.M. Biesheuvel, H. Miedema, H. Bruning, A.V.D. Wal, Charge Efficiency: A Functional Tool to Probe the Double-Layer Structure Inside of Porous Electrodes and Application in the Modeling of Capacitive Deionization, *Journal of Physical Chemistry Letters*, 1 (2010) 205-210.
- [13] Z.U. Khan, T.T. Yan, L.Y. Shi, D.S. Zhang, Improved capacitive deionization by using 3D intercalated graphene sheet-sphere nanocomposite architectures, *Environ.-Sci. Nano*, 5 (2018) 980-991.
- [14] X. Wu, X. Hong, Z. Luo, K.S. Hui, H. Chen, J. Wu, K.N. Hui, L. Li, J. Nan, Q. Zhang, The effects of surface modification on the supercapacitive behaviors of novel mesoporous carbon derived from rod-like hydroxyapatite template, *Electrochim. Acta*, 89 (2013) 400-406.

- [15] Z.Q. Hao, J.P. Cao, Y. Wu, X.Y. Zhao, Q.Q. Zhuang, X.Y. Wang, X.Y. Wei, Preparation of porous carbon sphere from waste sugar solution for electric double-layer capacitor, *J. Power Sources*, 361 (2017) 249-258.
- [16] C. Tsouris, R. Mayes, J. Kiggans, K. Sharma, S. Yiacoumi, D. Depaoli, S. Dai, Mesoporous Carbon for Capacitive Deionization of Saline Water, *Environmental Science & Technology*, 45 (2011) 10243.
- [17] C.-C. Huang, J.-C. He, Electrosorptive removal of copper ions from wastewater by using ordered mesoporous carbon electrodes, *Chem. Eng. J.*, 221 (2013) 469-475.
- [18] L.M. Chang, X.Y. Duan, W. Liu, Preparation and electrosorption desalination performance of activated carbon electrode with titania, *Desalination*, 270 (2011) 285-290.
- [19] Y. Yao, B. Gao, J. Chen, L. Yang, Engineered biochar reclaiming phosphate from aqueous solutions: mechanisms and potential application as a slow-release fertilizer, *Environmental Science & Technology*, 47 (2013) 8700-8708.
- [20] M.P. Bernardo, F.K.V. Moreira, C. Ribeiro, Synthesis and characterization of eco-friendly Ca-Al-LDH loaded with phosphate for agricultural applications, *Appl. Clay Sci.*, 137 (2017) 143-150.
- [21] K.H. Goh, T.T. Lim, Z. Dong, Application of layered double hydroxides for removal of oxyanions: A review, *Water Res.*, 42 (2008) 1343-1368.
- [22] P.P. Huang, C.Y. Cao, F. Wei, Y.B. Sun, W.G. Song, MgAl layered double hydroxides with chloride and carbonate ions as interlayer anions for removal of arsenic and fluoride ions in water, *RSC Adv.*, 5 (2015) 10412-10417.
- [23] H.N. Tran, C.C. Lin, H.P. Chao, Amino acids-intercalated Mg/Al layered double hydroxides

as dual-electronic adsorbent for effective removal of cationic and oxyanionic metal ions, *Sep. Purif. Technol.*, 192 (2018) 36-45.

[24] S. Wan, S.S. Wang, Y.C. Li, B. Gao, Functionalizing biochar with Mg-Al and Mg-Fe layered double hydroxides for removal of phosphate from aqueous solutions, *J. Ind. Eng. Chem.*, 47 (2017) 246-253.

[25] R.H. Li, J.J. Wang, B.Y. Zhou, M.K. Awasthi, A. Ali, Z.Q. Zhang, L.A. Gaston, A.H. Lahori, A. Mahar, Enhancing phosphate adsorption by Mg/Al layered double hydroxide functionalized biochar with different Mg/Al ratios, *Sci. Total Environ.*, 559 (2016) 121-129.

[26] J. Das, B.S. Patra, N. Baliarsingh, K.M. Parida, Adsorption of phosphate by layered double hydroxides in aqueous solutions, *Appl. Clay Sci.*, 32 (2006) 252-260.

[27] T.R. Zhan, Y.M. Zhang, Q. Yang, H.H. Deng, J. Xu, W.G. Hou, Ultrathin layered double hydroxide nanosheets prepared from a water-in-ionic liquid surfactant-free microemulsion for phosphate removal from aquatic systems, *Chem. Eng. J.*, 302 (2016) 459-465.

[28] Y. Wang, W.S. Yang, S.C. Zhang, D.G. Evans, X. Duan, Synthesis and electrochemical characterization of Co-Al layered double hydroxides, *J. Electrochem. Soc.*, 152 (2005) A2130-A2137.

[29] M. Zhang, B. Gao, Y. Yao, M. Inyang, Phosphate removal ability of biochar/MgAl-LDH ultra-fine composites prepared by liquid-phase deposition, *Chemosphere*, 92 (2013) 1042-1047.

[30] D. Huang, J. Ma, L. Yu, D. Wu, K. Wang, M. Yang, D. Papoulis, S. Komarneni, AgCl and BiOCl composited with NiFe-LDH for enhanced photo-degradation of Rhodamine B, *Sep. Purif. Technol.*, 156 (2015) 789-794.

[31] K. Yang, L.G. Yan, Y.M. Yang, S.J. Yu, R.R. Shan, H.Q. Yu, B.C. Zhu, B. Du, Adsorptive

removal of phosphate by Mg-Al and Zn-Al layered double hydroxides: Kinetics, isotherms and mechanisms, *Sep. Purif. Technol.*, 124 (2014) 36-42.

[32] L. Lupa, L. Cochechi, R. Pode, I. Hulka, Phenol adsorption using Aliquat 336 functionalized Zn-Al layered double hydroxide, *Sep. Purif. Technol.*, 196 (2018) 82-95.

[33] C.Y. Zhang, D. He, J.X. Ma, W.W. Tang, T.D. Waite, Faradaic reactions in capacitive deionization (CDI) - problems and possibilities: A review, *Water Res.*, 128 (2018) 314-330.

[34] J.J. Wouters, M.I. Tejedor-Tejedor, J.J. Lado, R. Perez-Roa, M.A. Anderson, Influence of Metal Oxide Coatings, Carbon Materials and Potentials on Ion Removal in Capacitive Deionization, *J. Electrochem. Soc.*, 165 (2018) E148-E161.

[35] T.T. Yan, J. Liu, H. Lei, L.Y. Shi, Z.X. An, H.S. Park, D.S. Zhang, Capacitive deionization of saline water using sandwich-like nitrogen-doped graphene composites via a self-assembling strategy, *Environ.-Sci. Nano*, 5 (2018) 2722-2730.

[36] J. Liu, M. Lu, J. Yang, J. Cheng, W. Cai, Capacitive desalination of ZnO/activated carbon asymmetric capacitor and mechanism analysis, *Electrochim. Acta*, 151 (2015) 312-318.

[37] X. Peng, X. Hu, D. Fu, F.L.Y. Lam, Adsorption removal of acid black 1 from aqueous solution using ordered mesoporous carbon, *Applied Surface Science*, 294 (2014) 71-80.

[38] J.B. Lu, H.J. Liu, X. Zhao, W. Jefferson, F. Cheng, J.H. Qu, Phosphate removal from water using freshly formed Fe-Mn binary oxide: Adsorption behaviors and mechanisms, *Colloid Surf. A-Physicochem. Eng. Asp.*, 455 (2014) 11-18.

[39] H. Zhang, R. Qi, X. Duan, Studies on structures and properties of MgAl and MgFe layered double hydroxides, *Chinese Journal of Inorganic Chemistry*, 18 (2002) 833-838.

[40] J. Zhang, J.H. Fang, J.L. Han, T.T. Yan, L.Y. Shi, D.S. Zhang, N, P, S co-doped hollow

carbon polyhedra derived from MOF-based core-shell nanocomposites for capacitive deionization,

*J. Mater. Chem. A*, 6 (2018) 15245-15252.

[41] J.L. Han, L.Y. Shi, T.T. Yan, J.P. Zhang, D.S. Zhang, Removal of ions from saline water using N, P co-doped 3D hierarchical carbon architectures via capacitive deionization, *Environ.-Sci. Nano*, 5 (2018) 2337-2345.

[42] K.S. Triantafyllidis, E.N. Peleka, V.G. Komvokis, P.P. Mavros, Iron-modified hydroxalcalite-like materials as highly efficient phosphate sorbents, *J. Colloid Interface Sci.*, 342 (2010) 427-436.

[43] X.R. Ma, H.J. Li, G. Zhu, L.P. Kang, Z.H. Liu, Hydrothermal preparation and anion exchange of  $\text{Co}^{2+}$ - $\text{Ni}^{2+}$ - $\text{Fe}^{3+}$   $\text{CO}_3^{2-}$  LDHs materials with well regular shape, *Colloid Surf. A-Physicochem. Eng. Asp.*, 371 (2010) 71-75.

[44] A.M. Kiss, T.D. Myles, K.N. Grew, A.A. Peracchio, G.J. Nelson, W.K.S. Chiu, Carbonate and Bicarbonate Ion Transport in Alkaline Anion Exchange Membranes, *J. Electrochem. Soc.*, 160 (2013) F994-F999.

[45] M. Xie, M. Zheng, P. Cooper, W.E. Price, L.D. Nghiem, M. Elimelech, Osmotic dilution for sustainable greenwall irrigation by liquid fertilizer: Performance and implications, *J. Membr. Sci.*, 494 (2015) 32-38.

[46] C.V. Luengo, M.A. Volpe, M.J. Avena, High sorption of phosphate on Mg-Al layered double hydroxides: Kinetics and equilibrium, *J. Environ. Chem. Eng.*, 5 (2017) 4656-4662.

[47] N. Iyi, T. Sasaki, Decarbonation of MgAl-LDHs (layered double hydroxides) using acetate-buffer/NaCl mixed solution, *J. Colloid Interface Sci.*, 322 (2008) 237-245.

[48] F.Z. Xie, F.C. Wu, G.J. Liu, Y.S. Mu, C.L. Feng, H.H. Wang, J.P. Giesy, Removal of

Phosphate from Eutrophic Lakes through Adsorption by in Situ Formation of Magnesium Hydroxide from Diatomite, *Environmental Science & Technology*, 48 (2014) 582-590.

[49] K.W. Jung, S. Lee, Y.J. Lee, Synthesis of novel magnesium ferrite (MgFe<sub>2</sub>O<sub>4</sub>)/biochar magnetic composites and its adsorption behavior for phosphate in aqueous solutions, *Bioresource technology*, 245 (2017) 751-759.

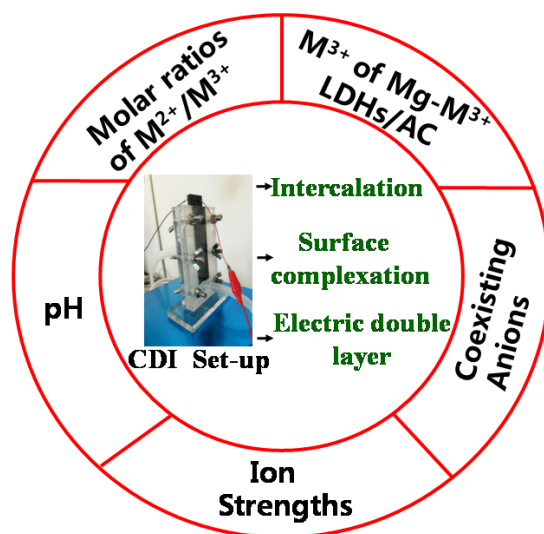
[50] X.L. Wu, X.L. Tan, S.T. Yang, T. Wen, H.L. Guo, X.K. Wang, A.W. Xu, Coexistence of adsorption and coagulation processes of both arsenate and NOM from contaminated groundwater by nanocrystalline Mg/Al layered double hydroxides, *Water Res.*, 47 (2013) 4159-4168.

[51] H.B. Li, S. Liang, M.M. Gao, G.L. Li, J. Li, L.J. He, The study of capacitive deionization behavior of a carbon nanotube electrode from the perspective of charge efficiency, *Water Sci. Technol.*, 71 (2015) 131-136.

[52] N. Pugazhentiran, S.S. Gupta, A. Prabhath, M. Manikandan, J.R. Swathy, V.K. Raman, T. Pradeep, Cellulose Derived Graphenic Fibers for Capacitive Desalination of Brackish Water, *ACS Appl. Mater. Interfaces*, 7 (2015) 20156-20163.

[53] Y. He, H. Lin, Y. Dong, L. Wang, Preferable adsorption of phosphate using lanthanum-incorporated porous zeolite: Characteristics and mechanism, *Applied Surface Science*, 426 (2017) 995-1004.

Graphical abstract



Influence of various parameters on capacitive removal of phosphate on LDHs/AC electrode

**Highlights:**

- ▶ The high phosphate adsorption capacity reach 80.43 mg/g for 250 mg·L<sup>-1</sup> KH<sub>2</sub>PO<sub>4</sub> solution.
- ▶ An optimization of preparation conditions and important operating parameters are provided.
- ▶ The uptake of phosphate by Mg-Al LDHs/AC under circumneutral pH reach maximum uptake level.
- ▶ The ionic strength mainly affects the CDI by the electric double layer instead of intercalation.